DR. RONGTING XU (Orcid ID : 0000-0001-7292-9271)

DR. HANQIN TIAN (Orcid ID : 0000-0003-2019-9603)

DR. JIA YANG (Orcid ID : 0000-0003-2019-9603)

Article type : Primary Research Articles

Global ammonia emissions from synthetic nitrogen fertilizer applications in agricultural systems: empirical and process-based estimates and uncertainty

Rongting Xu[1], Hanqin Tian[1,2], Shufen Pan[1], Stephen A. Prior[3], Yucheng Feng[4], William D. Batchelor[5], Jian Chen[6,1] and Jia Yang[1,2]

[1]International Center for Climate and Global Change Research, School of Forestry and Wildlife Sciences, Auburn University, USA

[2]Research Center for Eco-Environmental Sciences, Chinese Academy of Sciences, State Key Laboratory of Urban and Regional Ecology, Beijing 100085, China

[3]USDA-ARS National Soil Dynamics Laboratory, USA

[4]Department of Crop, Soil and Environmental Sciences, Auburn University, USA

[5]Department of Biosystems Engineering, Auburn University, USA

[6]Department of Computer Science and Software Engineering, Samuel Ginn College of Engineering, Auburn University, USA

* Correspondence: Hanqin Tian, email: tianhan@auburn.edu

Running head: Global ammonia emissions

Paper type: Primary Research Articles

Abstract

Excessive ammonia (NH_3) emitted from nitrogen (N) fertilizer applications in global croplands plays an important role in atmospheric aerosol production, resulting in visibility reduction and regional haze. However, large uncertainty exists in NH_3 emission estimates from global and regional croplands, which utilize different data and methods. In this study, we have coupled a process-based Dynamic Land Ecosystem Model (DLEM) with the bi-directional NH_3 exchange module in the Community Multiscale Air-Quality (CMAQ) model (DLEM-Bi-NH_3) to quantify NH_3 emissions at the global and regional scale, and crop-specific NH_3 emissions globally at a spatial resolution of 0.5° × 0.5° during 1961–2010. Results indicate that global NH_3 emissions from N fertilizer use have increased from 1.9±0.03 to 16.7±0.5 Tg N yr^{-1} between 1961 and 2010. The annual increase of NH_3 emissions shows large spatial variations across the global land surface. Southern Asia, including China and India, has accounted for more than 50% of total global NH_3 emissions since the 1980s, followed by North America and Europe. Rice cultivation has been the largest contributor to total global NH_3 emissions since the 1990s, followed by corn and wheat. In addition, results show that empirical methods without considering environmental factors (constant emission factor in the IPCC Tier 1 guideline) could underestimate NH_3 emissions in the context of climate change, with the highest difference (i.e., 6.9 Tg N yr^{-1}) occurring in 2010. This study provides a robust estimate on global and regional NH_3 emissions over the past 50 years, which offers a reference for policy-makers and farmers to optimally manage nitrogen fertilizer practices for compromising air quality and food security.

Keywords: ammonia, aerosol, nitrogen fertilizer, emission factors, agricultural systems

Introduction

Over the past century, a large quantity of chemical N fertilizer was produced using the Haber-Bosch process that converts atmospheric dinitrogen gas (N_2) to ammonia (NH_3). Mineral fertilizer application in cropland contributed to the rapid increase in food production, which supported the fast global population growth (Erisman *et al.*, 2008, Gruber & Galloway, 2008). Human-caused reactive N (typically from agricultural systems) was at least twice the rate of naturally created terrestrial N in 2010 (Ciais *et al.*, 2014). These excess reactive N compounds in terrestrial ecosystems play a role in the emission of N-containing gases, including oxides of nitrogen (N_2O and NO_x), and NH_3 (Tian *et al.*, 2016). The high output of these N-containing gases remains a matter of great concern to human and environmental health (Behera *et al.*, 2013).

Agricultural activities account for approximately 80~90% of total anthropogenic NH_3 emissions (Bouwman *et al.*, 1997, Zhang *et al.*, 2010). There are two major sources for NH_3 emissions: volatilization from livestock manure and mineral fertilizer application (Asman *et al.*, 1998, Bouwman *et al.*, 1997). A large amount of NH_3 from synthetic N fertilizer is lost to the atmosphere where short-distance transport can return it to the land by wet or dry deposition (Asman *et al.*, 1998). With substantial increases in manure production and chemical N fertilizer consumption, deposition of reactive N has increased across many regions of the globe. For example, the average atmospheric N deposition in this century was twenty-fold higher than that in the pre-industrial period (Dentener, 2006). This increased N deposition has contributed to eutrophication, acidification, and loss of biodiversity in the global ecosystem (Erisman *et al.*, 2008). Moreover, NH_3 is one of key precursors for aerosol ($PM_{2.5}$) formation in the atmosphere that could adversely affect respiratory and cardiovascular systems, and contribute to visibility reduction and regional haze (Pinder *et al.*, 2007, Seinfeld & Pandis, 1998). For these reasons, a robust understanding of the magnitude and spatiotemporal patterns of global NH_3 emissions from agricultural activities is essential.

This study mainly focused on NH_3 emissions from synthetic N fertilizer application. Mineral N fertilizer contributed 10–15% of the total estimated NH_3 emissions (45~75 Tg N annually) from terrestrial ecosystems at the end of the last century (Matthews, 1994). Bouwman *et al.* (1997) estimated global NH_3 emissions in 1990 as ~54 Tg N yr^{-1} with synthetic N fertilizer application accounting for ~16.7% (9 Tg N yr^{-1}). This estimate was comparable to the 8.5 Tg N

yr^{-1} of Schlesinger and Hartley (1992). Riddick *et al.* (2016) provided an estimate of global NH_3 emission of 12 Tg N yr^{-1} from N fertilizer for the year 2000. Previous studies have mainly focused on one-year annual NH_3 emission estimates. Although Riddick *et al.* (2016) presented seasonal estimates of global NH_3 emissions, their simplification of agricultural practices (e.g., no double cropping) along with not considering rice cultivations introduces large uncertainties in their seasonal estimates. Thus, studies of global inter-annual and crop-specific NH_3 emissions are still needed.

Emission factors (EF) and process-based models are two major approaches for quantifying global or regional NH_3 emissions from N fertilizer use. The EF represents the percentage of applied N fertilizer that volatilizes as NH_3, which varies with synthetic N fertilizer types. Constant values are often assumed for EFs used to build emission inventories at the global and regional scale, such as the Emission Database for Global Atmospheric Research (EDGAR, Olivier *et al.*, 2002) and the National Emission Inventory (NEI, Reis *et al.*, 2009) of the United States. Numerous efforts have been made to determine EFs for NH_3 emissions at the regional scale (e.g., Europe, United States, and China). However, robust estimations at the global scale and on crop-specific NH_3 emissions globally over historical time series are lacking. Moreover, large uncertainties still exist for monthly and annual NH_3 emission estimates in previous studies (Riddick *et al.*, 2016, Xu *et al.*, 2016, Zhou *et al.*, 2016). The most widely applied EF of 10% was reported in the Intergovernmental Panel on Climate Change (IPCC) Tier 1 guidelines. Other studies provided global mean EFs ranging from 14 to 21% (Beusen *et al.*, 2008, Bouwman *et al.*, 2002, FAO & IFA report, 2001). However, these studies based on constant EFs were one-year estimates that did not consider how NH_3 emissions respond to climate change and variability.

Process-based models are another popular approach for estimating NH_3 emissions. For instance, the bi-directional NH_3 exchange module has been incorporated into the US Environmental Protection Agency's (EPA) Community Multiscale Air-Quality model (CMAQ, Byun & Schere, 2006) and coupled with the United States Department of Agriculture's (USDA) Environmental Policy Integrated Climate (EPIC) agroecosystem model (Bash *et al.*, 2013, Massad *et al.*, 2010, Nemitz *et al.*, 2000) to estimate seasonal and annual NH_3 emissions from synthetic N fertilizer applications. The Flow of Agricultural Nitrogen (FAN) process model has been combined within the Community Land Model 4.5 to compute the reactive N flows and NH_3

emissions (Riddick *et al.*, 2016). Our previous study incorporated the bi-directional NH_3 exchange module in CMAQ within the Dynamic Land Ecosystem Model (DLEM, Tian *et al.*, 2011) (DLEM-Bi-NH_3) and applied this model to estimate NH_3 emissions from Asian agricultural systems for 1961–2014 (Xu *et al.*, 2018).

The current study applied the DLEM-Bi-NH_3 module to estimate NH_3 emissions from synthetic N fertilizer application in global croplands from 1961 to 2010. The objectives of this paper were to: (1) investigate spatial and temporal variations of NH_3 emissions; (2) examine the impact of climate factors on NH_3 emissions driven by four historical climate datasets; (3) analyze crop-specific NH_3 emissions from global croplands; and (4) compare global NH_3 emissions from model simulations with estimates from EFs in the IPCC Tier 1 guideline.

Materials and methods

General description of the DLEM model

The DLEM model is a highly integrated process-based ecosystem model that makes daily, spatially-explicit estimates of carbon, nitrogen and water fluxes and pool sizes within both natural and human-dominant ecosystems, and also simulates the exchanges of major greenhouse gases (GHGs) between terrestrial ecosystems and the atmosphere at site, regional, and global scales (Tian *et al.*, 2011, 2015). This is accomplished by combining five model components: 1) biophysical characteristics, 2) plant physiological processes, 3) soil biogeochemical cycles, 4) vegetation dynamics, and 5) land use and disturbances. Biophysical characteristics component simulates water and energy fluxes in terrestrial ecosystems and their interactions with the environment. The plant physiological process component simulates all essential processes of plant growth, such as photosynthesis, respiration, allocation, and evapotranspiration. The biogeochemical cycle processes component includes processes of decomposition, nitrogen mineralization/immobilization, nitrification/denitrification, fermentation, and other major biochemical processes in soils. The land use and disturbance component simulates the impact of natural and human disturbances on water and nutrient fluxes and storages in the land biosphere. Daily crop growth and trace gas exchanges between agroecosystems and the atmosphere is also simulated in the agricultural module of DLEM (DLEM-AG). The model is also capable of

estimating crop productivity (net primary production) and yield. Detailed descriptions of DLEM-AG can be found in Ren *et al.* (2011) and Tian *et al.* (2012a, 2015).

Greenhouse gas (GHG) emissions estimated by DLEM model have been validated against field observations and measurements at various sites in the historical period (Lu & Tian, 2013, Tian *et al.*, 2010, Tian *et al.*, 2011, Xu *et al.*, 2017). The DLEM model has also been used to predict GHG emissions, carbon and nutrient fluxes, and global net primary production driven by climate data obtained from several General Circulation Models for the period 2011−2099 (Pan *et al.*, 2014, Ren *et al.*, 2015, Tian *et al.*, 2012b). Simulated results of water, carbon, and nutrients fluxes and storages derived from DLEM model were also compared with estimates from various approaches at regional, continental, and global scales (Tian *et al.*, 2015, Yang *et al.*, 2015). These previous efforts demonstrate that DLEM model can realistically simulate the biogeochemical cycles in soils at various spatiotemporal scales.

Description of the DLEM-Bi-NH_3 module

In the DLEM model, NH_4^+ inputs (e.g., synthetic N fertilizer) to soils are subjected to NH_3 volatilization, plant and microbial uptake, nitrification, and N leaching that result in variable amounts of NH_4^+ over time. In detail, soil NH_4^+ decreases due to soil immobilization, nitrification, anaerobic ammonium oxidation, NH_3 volatilization, organic and inorganic N leaching and runoff, while NH_4^+ increases due to soil mineralization, biological N_2 fixation, nitrate ammonification, N deposition, and fertilizer/manure N application. These processes are regulated by environmental factors (e.g., soil temperature, moisture, pH) and vegetation (e.g., crop type, NH_4^+ uptake). Different soil organic pools and decomposition processes, and how they affect NH_4^+ budgets in soils can be found in Tian *et al.* (2015) and Xu *et al.* (2018). The NH_3 volatilization process described in the DLEM-Bi-NH_3 module can affect crop growths as well as other N-involving processes within agricultural soils in the DLEM model after synthetic N fertilizer was applied (see Text S1).

In the DLEM-Bi-NH_3 module, the overall emission flux of NH_3 (F_{emis}) varies daily after synthetic N fertilizer was applied to soils and is calculated as follows:

$$F_{emis} = C_c / (R_a + 0.5\, R_{inc}) \quad (1)$$

where C_c is the canopy NH_3 compensation point, R_a is aerodynamic resistance, and R_{inc} is aerodynamic resistance within the canopy. Ammonia fluxes are given in μg m^{-3} s^{-1}, while units for all compensation points and the above resistances are μg m^{-3} and s m^{-1}, respectively. Other major equations of the DLEM-Bi-NH_3 module can be found in Supplementary Material and Xu *et al.* (2018). The DLEM-Bi-NH_3 module has been validated using field observations at multiple sites globally (see Table S2 in Xu *et al.* (2018)).

In this study, we considered 10 crop types including rice, corn, wheat, soybean, cotton, millet, sorghum, groundnuts, barley, and rapeseed globally. In addition, we included different crop rotation systems (e.g., rice-wheat, rice-rice, corn-wheat, and soybean-wheat). Fertilizer timings were determined based on previous literatures (see Text S1 in Xu *et al.* (2018) and Text S2 & Table S1 of this study). While using the DLEM-Bi-NH_3 module, fertilizer application mainly consisted of adding NH_4^+ and was independent of fertilizer types. The pH value of soil after N fertilizer application was taken as 7.5 (Massad *et al.*, 2010). Fertilizer application methods (e.g., basal or topdressing) were not considered in this study. We assumed fertilizer remains at the surface layer (top 5 cm) when applied to soils (Massad *et al.*, 2010). In reality, emissions are sensitive to fertilizer types (e.g., Yan *et al.*, 2003, Zhou *et al.*, 2016), to pH value (e.g., Sommer & Olesen, 1991), and to specific agricultural practices (e.g., Fu *et al.*, 2015, Ju *et al.*, 2009, Zhou *et al.*, 2016). It is very likely that these factors might reduce NH_3 emission estimates.

Input data description

Input datasets for the DLEM-Bi-NH_3 simulations include a natural vegetation map, land use change (LUC), synthetic N fertilizer application, atmospheric CO_2 concentration, and time series of climate at a spatial resolution of 0.5° × 0.5°. The developed natural vegetation map was based on SYNMAP (Jung *et al.*, 2006), which rendered fractions of 47 vegetation types in each 0.5° grid. These 47 vegetation types were converted to 15 plant functional types for use in the DLEM through a cross-walk table with a spatial pattern that can be found in Pan *et al.* (2015) and Xu *et al.* (2017). Cropland distribution datasets were developed by aggregating 5-arc minute resolution HYDE v.3.2 global cropland distribution data (Klein Goldewijk *et al.*, 2017) to the resolution of 0.5° × 0.5° latitude/longitude. Spatially-explicit LUC data for 1900–2005 was retrieved from high-resolution remotely sensed data, field surveys and contemporary LUC patterns reported in

China's National Land Cover Datasets (Liu & Tian, 2010, Lu *et al.*, 2012, Ren *et al.*, 2012); this dataset has been updated to the year 2010. The land-use change dataset for India was developed from remote sensing datasets available from the Advanced Wide-Field Sensor of Resourcesat-1 during 2005–2009 in combination with three inventory datasets during 1880–2010 to reconstruct LUC at 5-arc minute resolution during 1880–2010 (Tian *et al.*, 2014). Land-use change datasets of China and India were aggregated to 0.5° to replace HYDE v.3.2 for both regions from 1900 to 2010. Cropland spatial distribution within each grid for 1961 and 2010 are shown in Figure S1. A spatially-explicit time-series dataset of agricultural N fertilizer use was developed through spatializing IFA-based country-level N fertilizer consumption according to crop specific N fertilizer application rates, crop type distribution, and historical cropland distribution during 1960–2013 (Lu & Tian, 2017).

Half-degree daily climate data (e.g., average, maximum, minimum air temperature, precipitation, relative humidity, and shortwave radiation) were derived from CRUNCEP climate forcing data (Wei *et al.*, 2013). Long-term average climate datasets (1901 to 1930) were used to represent the initial climate state in 1900. Three additional climate datasets (PGMFD v.2, GSWP3, and WFDEI_WFDEI) with 0.5° × 0.5° resolution of daily climate data were obtained from the Inter-Sectoral Impact Model Integration and Intercomparison Project (ISI-MIP 2.1). All data are available at the ISI-MIP website (www.isimip.org). The monthly CO_2 concentration dataset obtained from NOAA extended GLOBALVIEW-CO_2 spanned the time period of 1900 to 2010 (http://www.esrl.noaa.gov/gmd/ccgg/globalview/co2/).

Model simulation experiments and implementation

Six simulation experiments were conducted to achieve our objectives. Implementation of the DLEM-Bi-NH_3 simulation included three steps: (1) equilibrium run, (2) spin-up run, and (3) transient run. All datasets that used to drive the model in the equilibrium run were in 1900. The equilibrium state was assumed to reach when intra-annual variations of carbon, nitrogen, and water storage were less than 0.1 g C/m^2, 0.1 g N/m^2 and 0.1 mm, respectively, during two consecutive 50 years in each grid. The long-term mean climate data for 1901 to 1930 were used to represent 1900 climate. Following the equilibrium run, the model was spun-up by de-trended climate data (1901 to 1930) to allow smoother model mode transitions from equilibrium runs to transient runs more smoothly (i.e., three spins with 10-year climate data each time). Finally, the

model was run in the transient mode using daily climate data, CO_2 concentration, N fertilizer application, and LUC inputs for the 1901 to 2010 time period. We conducted three simulation experiments (S1, S2, and S3) driven by CRUNCEP climate forcing data to investigate the response of global NH_3 emissions to temperature and precipitation changes in the historical period (Table 1). The difference in NH_3 emissions simulated by S3 and S1 experiments refers to the climate effects: the difference between S2 and S1 experiments reflected temperature effects and precipitation effects was from the difference between S3 and S2 experiments. To estimate the NH_3 emission response to different climate datasets, four simulation experiments (S3–S6) were conducted, driven by different climate datasets during 1901–2010.

Results

Temporal changes in global NH_3 emissions

We quantified NH_3 emissions from global croplands associated with synthetic N fertilizer application during 1961–2010. Model simulations showed a significant increase in annual mean global NH_3 emissions (Fig. S2). Compared to the 1960s (2.8±1.5 Tg N yr^{-1}), we estimated an increase of 12.0±0.8 Tg N yr^{-1} (436%) in NH_3 emissions associated with a 71.4 Tg N yr^{-1} increase in mean N fertilizer applied to croplands in the 2000s driven by four different climate datasets (S3–S6). Error bars, ±2 standard deviation (s.d.) calculated from simulation results based on four different climate datasets. The highest global mean NH_3 emission was estimated at 16.7±0.5 Tg N yr^{-1} in 2010. Total NH_3 emissions associated with different climate datasets varied with a maximum value for WFDEI.GPCC (17.0 Tg N yr^{-1}) and a minimum value for CRUNCEP (16.5 Tg N yr^{-1}) in 2010. Global NH_3 emissions positively responded to increased N fertilization whose temporal trends were similar to N fertilizer input trends. Thus, although climate is an important factor that affects NH_3 emissions from global croplands, the rapid increase in synthetic N fertilizer applications was the more dominant factor impacting the rise in global NH_3 emissions in the past half-century.

Spatial pattern of global NH_3 emissions

Ammonia emissions varied widely across countries and regions. The magnitude of differences between regions became larger with the increase in global N fertilizer-induced NH_3 emissions during 1961–2010 (Fig. S3). In the 1960s, major sources were North America and Europe, which

contributed to 70% of total annual emissions at an estimated rate of 0.3 to 0.5 g N m^{-2} yr^{-1} (Fig. 1). Emission rates from remaining grids of different continents stayed within 0~0.05 g N m^{-2} yr^{-1}. In the 1980s and 1990s, a large NH_3 emission increases were found in all continents of the Northern Hemisphere, especially in southern Asia, where NH_3 emission rates were as high as 1.5~2.0 g N m^{-2} yr^{-1}. Total contributions from North America and Europe was 43.2% in the 1980s and 34.2% in the 1990s. The largest variation in spatial patterns were in the 2000s (Fig. 1). Southern Asia contributed 61.1% of total emissions. The highest emission rate was found in the North Plain of China, which was greater than 3.0 g N m^{-2} yr^{-1} (Fig. S3). With expansion of cropland and increased N fertilizer consumption in the Southern Hemisphere, all continents showing substantial increases in NH_3 emission rates (within a mean range of 0~0.05 g N m^{-2} yr^{-1} in the 1960s) shifted to a range of 1.0~1.5 g N m^{-2} yr^{-1} in the 2000s.

From a continental perspective, North America, Europe, and southern Asia were the three major NH_3 emissions regions in the 1960s (i.e., 1.0±0.5, 0.9±0.4, and 0.6±0.5 Tg N yr^{-1}, respectively). Only Europe showed a declining emission trend since the 1980s, with a mean decrease rate of ~0.6 Gg N yr^{-1} (1Gg = 1×10^{-3} Tg). The decadal change in NH_3 emissions from North America was slight since the 1980s. In contrast, southern Asia became the leading emitter with a mean increase rate of ~225.8 Gg N yr^{-1} during 1980–2010 (Fig. 2). In the 1960s, NH_3 emissions from South America, Africa, and Oceania were 0.06±0.05, 0.08±0.04, and 0.014±0.012 Tg N yr^{-1}, respectively. South America and Africa showed a large increase in NH_3 emissions since the 1990s, with a mean rate of ~42.4 and ~10 Gg N yr^{-1}, respectively. Oceania showed an increasing trend with a mean rate of ~7.5 Gg N yr^{-1}. Ammonia emissions have been highly concentrated since 1988, with more than 50% of emissions sourced from southern Asia. The highest emission in North America, southern Asia, and Europe was estimated as 2.46±0.09 in 1991, 10.21±0.5 in 2009, and 2.30±0.03 Tg N yr^{-1} in 1990, respectively.

Intra-annual changes of global and regional NH_3 emissions

In terms of intra-annual variation, we only focused on emissions in the 2000s driven by one climate dataset (CRUNCEP). There were two peaks (March–April–May and June–July–August) of global NH_3 emissions from N fertilizer applications during 2000–2010 (Fig. S4), which contributed about 72% of total N fertilizer-induced emissions. In contrast, December–January–February contributed least and accounted for less than 10% of total

emissions. The NH_3 emissions during June–July–August showed an increasing trend during 2000–2010. Meanwhile, the seasonal contribution of NH_3 emissions varied for the different continents (Fig. 3). In Asia, the estimated NH_3 emissions in winter (December to February), spring (March to May), summer (June to August), and autumn (September to November) accounted for 5.9%, 22.2%, 56.6%, 15.3% of the annual emission, respectively. In North America, the estimated NH_3 emissions in winter, spring, summer, and autumn accounted for 3.7%, 64.9%, 19.2%, 12.2% of the annual emission, respectively. In Europe, the estimated NH_3 emissions in winter, spring, summer, and autumn accounted for 1.6%, 63.2%, 0.3%, 34.9% of the annual emission, respectively.

From December to February, regions close to the tropics (±30°) were significant sources of NH_3 emissions (e.g., Northeast and South India, South Africa, and Brazil; Fig. 3). From March to May, the emissions shifted to the Northern Hemisphere, where North America, Europe, and southern Asia were the largest sources of global NH_3 emission; this was especially true for the Midwestern United States, Europe, North Plain of China, and North India (Fig. 3). In addition, regions within the northern tropics acted as NH_3 sources (e.g., Mexico and Southeast Asia). In summer, the Northern Hemisphere continuously acted as the largest NH_3 source. Moreover, NH_3 emissions were substantial in the entire area of India and the North, Northeast, and Southeast Plain of China, and most countries in Southeast Asia. However, there was a slight emission associated with Europe and the Midwestern United States. From September to November, NH_3 emissions covered all continents of the Earth's surface.

Crop-specific NH_3 emissions

From a crop-type perspective, we identified four major global crops (rice, corn, wheat, and soybean) and estimated NH_3 emissions from these crops due to synthetic N fertilizer application during 1961–2010. These four crops accounted for 67% of the total emission during the 1960s, among which wheat and corn were the two main sources (Fig. 4). In the 2000s, the largest source of NH_3 emissions was from rice (23.5%), followed by wheat (22.8%), and corn (21.9%) (Fig. 4). Soybean only accounted for less than 10% of the global annual total NH_3 emissions from 1961 to 2010 (Fig. 4). The transition of global NH_3 emissions from wheat and corn to rice, wheat, and corn was due to area expansion and increased fertilizer use in rice cultivation from 1961 to 2010 in the context of global warming.

Comparisons with the estimate by the IPCC Tier1 guideline methodology

The IPCC Tier1 guideline methodology used a constant EF of 10% to estimate global NH_3 emissions from synthetic N fertilizer use; i.e., emissions are equal to 10% of annual applied fertilizer amounts. Herein, global NH_3 emission from synthetic N fertilizer use was estimated to be 1.0 and 9.9 Tg N yr^{-1} in 1961 and 2010, respectively, based on the EF proposed in the IPCC Tier1 guideline methodology. In contrast, the simulated results from the DLEM in both years were nearly two times higher than the IPCC EF estimates (Fig. S2). The spatial patterns of EF-based results differed from those of our model simulations (Figs. 1 & S5). In the 1960s, NH_3 emissions from most regions based on DLEM simulations were slightly larger than IPCC EF estimates (mean range of 0–0.3 g N m^{-2} yr^{-1}) except for northern Europe and western United States. During the 1980s and 1990s, DLEM results were far larger than EF-based results in most regions across the globe (i.e., the upper and eastern Midwest of the United States and southern Asia, especially China, India, and Pakistan). The negative difference between EF-based and DLEM NH_3 emissions became much larger in some regions (i.e., northern and the upper eastern Europe, and the western United States) compared to differences in the 1960s. Also, negative differences appeared in western China (where most drylands are located), which was as low as 1.0 g N m^{-2} yr^{-1}. The largest difference in NH_3 emissions (i.e., per grid) appeared in the 2000s in northern India (> 5.0 g N m^{-2} yr^{-1}). In the Southern Hemisphere, DLEM results were continuously higher than IPCC EF estimates and the positive differences between these two approaches became larger during 1961–2010.

We compared crop-specific NH_3 emissions estimated by DLEM and IPCC EF during 1961–2010 (Fig. 4). Rice, wheat, and corn were three dominant crops responsible for the significant increase in NH_3 emissions from global croplands due to application of synthetic N fertilizer. Overall, DLEM NH_3 emissions from rice cultivation tended to increase faster than wheat and corn during 1961–2010 (Fig. S6). During the 1960s, the increasing rate of NH_3 emissions from rice, wheat, and corn according to DLEM were 0.83, 0.65, and 0.68 Tg N $decade^{-1}$, respectively. In contrast, the increased rate for these crops based on the IPCC EF was 0.43, 0.36, and 0.44 Tg N $decade^{-1}$, respectively.

Discussion

Comparisons with other studies

We compared our model results against previous studies based on EFs and process-based models at the global and regional scale. In our study, a general EF was calculated as modeled emissions divided by total N fertilizer applied across the global. At the global scale, the DLEM-simulated mean NH_3 emission in 2000 was 13.6±0.5 Tg N, which was ~14% higher than the FAN model estimates of Riddick *et al.* (2016) (Table 2). In comparison, the DLEM-simulated mean EF was 17.6%, which is slightly lower than their simulation (EF: 19%) in 2000. Although both studies are based on model simulations, our estimates are different for two major reasons: 1) model structures and parameters in both studies differed significantly; and 2) input datasets and fertilization timings were from various sources. For example, total synthetic N inputs and spatial patterns in our study were generated by Lu and Tian (2017), while Riddick *et al.* (2016) determined synthetic fertilizer application rates based on data provided by Potter *et al.* (2010). The estimated global NH_3 emission from synthetic N fertilizer was ~9 Tg N yr^{-1} in 1995 based on the EF calculated by Bouwman *et al.* (2002), which was 27% lower than our estimate (12.4 Tg N yr^{-1}; Table 2). Consequently, the estimated EF in Bouwman *et al.* (2002) was lower than the EF in our study for the same year. Differences between these studies were due to the synthetic N fertilizer dataset and estimate methodology. Generally, process-based model estimates of this study and previous estimate by Riddick *et al.* (2016) are higher than EF-based estimates (Table 2).

At the country scale, several studies have estimated NH_3 emissions from warm regions (e.g., China, India, and United States) using various approaches; however, there are large uncertainties with these estimates. Comparisons of estimated NH_3 emissions from synthetic N fertilizer applications in China and India from different studies were listed in Xu *et al.* (2018). Calculated 2002 NH_3 emissions in the United States (based on the CMAQ-EPIC model) were 73.68% lower than our estimates (Bash *et al.*, 2013). However, our 2008 estimate was similar to the NEI 2008 value (Rao *et al.*, 2013).

Climate effects on NH_3 emissions at spatiotemporal scales

By performing DLEM simulations based on four climate datasets from 1961–2010, we found that annual differences between various climate datasets were the primary factors affecting differences among simulation results. Annual estimates from CRUNCEP were lowest among all results driven by the other three climate forcing datasets. Additionally, differences rose with

increasing temperature during 1980–2010. Our simulated results show that climate effects on NH_3 emissions increased largely from 33.1 Gg N yr^{-1} in 1961 to 566.5 Gg N yr^{-1} in 2010, with substantial year-to-year variations. The average impact of climate variation is about 3%, ranging from 0% to 7% of annual total NH_3 emissions due to inter-annual variations during the period of 1961–2010. The increasing trend and variations in NH_3 is closely associated with increasing global annual temperature with large inter-annual variations. We found that annual NH_3 emissions increased with rising temperature and exhibited large inter-annual variations (Fig. 5). Temperature increase was a dominant factor that promoted climate effects in global NH_3 emissions. In most years, precipitation had a negative impact on increasing annual emissions to a small extent. This highlights the necessity to consider climate factors when estimating NH_3 emissions from agricultural soils.

Previous studies emphasized that NH_3 volatilization from N fertilizer application depends strongly on localized environmental factors; however, this impact has not been investigated at the global and regional scale, and on crop-specific emissions globally (Fu *et al.*, 2015, Huang *et al.*, 2012, Zhang *et al.*, 2011). Agricultural systems are complex due to the combination of human management and climate effects. Thus, process-based models could be an effective approach to address NH_3 exchange processes (Sutton *et al.*, 2013). However, the EF used in the IPCC Tier 1 guideline was a constant value regardless of regional variations affected by environmental factors. Our study provides comprehensive comparisons of crop-specific NH_3 emissions from global croplands between a constant EF and process-based models at the global and regional scale. Results showed that differences between the two approaches increased from 1.0 Tg N yr^{-1} to 6.9 Tg N yr^{-1} during 1961–2010. The largest positive difference was found in regions with warmer climates and/or with higher N fertilizer applications (e.g., southern Asia and North America; Fig. 4). Negative differences were found in regions with dry or cold climates (e.g., Northern Europe and western North America), which indicates that climate effects in these regions could retard NH_3 emissions. In our simulations, environmental factors (i.e., climate, soil properties, and cropland management strategies) were applied to simulate NH_3 emissions in each grid to better reflect NH_3 emission processes in real agricultural systems. Utilizing a constant EF without considering environmental factors could, to some extent, underestimate NH_3 emissions in the context of global warming. Similarly, Zhou *et al.* (2016) found that the estimated annual

404 NH_3 emission in China using a nonlinear model was 40% greater than that derived from the
405 IPCC Tier 1 guideline.

406 Crop-type scale comparisons demonstrated the importance of environmental impacts on NH_3
407 emissions. Our study provides evidence that NH_3 emissions were crop-type dependent and were
408 dominated by location and N fertilizer requirements. Crops such as barley grown at high
409 latitudes where temperatures were much lower than in the tropics contributed half of total
410 emissions compared to calculations based on the IPCC EF. In our study, emissions from rice-
411 cultivated regions (primarily in East, South, and Southeast Asia) were two times higher than
412 IPCC EF estimates and showed an increasing trend (Figs. 4 & S6). Although not the largest
413 receiver of global N fertilization in 2010 (Zhang *et al.*, 2015), rice was the top-ranking crop
414 contributing to global NH_3 emissions, followed by corn and wheat. A possible explanation is that
415 high temperature is the dominant factor that accelerates NH_3 emissions from rice cultivation.
416 However, Bouwman *et al.* (2002) mentioned that NH_3 volatilization from wetland rice systems
417 is complicated since it is dependent on rice height, aquatic biota growth that regulates floodwater
418 pH, and N fertilizer application timing and approaches.

419 Climate effects are of great importance and should be considered when estimating NH_3
420 emissions. By performing with/without climate and temperature-only simulations, we were able
421 to evaluate the contribution of different climate factors to the increase in global NH_3 emissions
422 during the historical period. Simulation results indicated that temperature was the dominant
423 factor behind increased emissions (Fig. 5).

424 ***Causes of intra-annual variations at regional scales***

425 Intra-annual NH_3 emissions are highly correlated to dates and N fertilizer application
426 amounts. Overall, rice, corn, and wheat received more than 50% of the world's synthetic N
427 fertilizer (Heffer, 2013) and were the three major NH_3 emission sources that account for ~65%
428 of total emissions during 1961–2010 in this study. In Asia, the estimated NH_3 emissions were
429 highest from summer (June to August), accounting for 56.6% of the annual emission. Higher
430 summer emissions were associated with cultivation periods and N fertilizer application timings
431 (see detailed description in Xu *et al.* (2018) Text S1). Rice cultivation areas in East, South, and
432 Southeast Asia contributed 89% of the world total (Yan *et al.*, 2003). In this study, rice fields
433 were the largest contributor to total Asian emissions since rice is the major cereal crop cultivated

in sub-tropical and tropical regions of Asia (East, South, and Southeast Asia) that use large amounts of fertilizer each summer (Aulakh *et al.*, 2001, Mahajan *et al.*, 2012, Zou *et al.*, 2005). For example, rice cultivation in China, India, Indonesia, Vietnam, Thailand, Bangladesh, and Philippines represented 16%, 30%, 45%, 60%, 45%, 83%, and 48% of total N fertilizer applied to all crops for each country, respectively (Heffer, 2013). As discussed above, warmer temperature during summer can stimulate NH_3 emissions in these regions thereby resulting in higher NH_3 emissions from fertilizer use.

In contrast, spring (March to May) accounted for about 60% of annual emissions in North America and Europe due to high fertilizer use for corn and winter/spring wheat. Corn is generally cultivated in April and May in northern mid-latitudes, winter wheat is usually planted in the fall (September and October), and spring wheat is generally planted in late spring (Sacks *et al.*, 2010, USDA NASS, 2010). We identified fertilizer timings according to field experiments, where N fertilizer was applied to corn and spring wheat at or before planting in spring, and the following March for winter wheat (Alluvione *et al.*, 2010, Guy & Gareau, 1998, Kunzová & Hejcman, 2009, Lopez-Bellido *et al.*, 2007). For example, corn and wheat cultivations represented 47% and 13%, respectively, of total N fertilizer applied to all crops in the United States, and 13% and 29%, respectively, of total N fertilizer applied to all crops in European countries (Heffer, 2013).

Uncertainties and future work

Although other studies focused on regional and global estimates of NH_3 emissions from synthetic N fertilizer application, large uncertainties associated with estimation approaches still remain. A process-based dynamic ecosystem model is a fundamental means to investigate agricultural system response to N fertilizer inputs as impacted by all environmental factors. Compared to static EFs in the IPCC Tier 1 guideline, results from our DLEM-Bi-NH_3 module could provide estimates of annual NH_3 emission fluctuations as affected by climate factors to better reflect real NH_3 volatilization processes. However, uncertainties in this study should be associated with N fertilizer datasets and timing of N fertilizer applications should be addressed in future work.

Ammonia volatilization from croplands is sourced from biological degradation of organic compounds and from synthetic and organic fertilizers yielding NH_4^+ (Bouwman *et al.*, 2002).

Thus, nitrogen fertilizer types can have significant impacts on NH_3 volatilization processes. As indicated in Nishina *et al.* (2017), synthetic N fertilizer consists of NH_4^+ and nitrate (NO_3^-), but the NH_4^+/ NO_3^- ratio in N fertilizer inputs shows obvious differences at spatiotemporal scales. Our study treated N fertilizer as a total input for NH_3 volatilization regardless of the fraction of NH_4^+ and did not distinguish N fertilizer type (Bash *et al.*, 2013, Fu *et al.*, 2015). In future studies, identifying N fertilizer types and treating them as different N sources would be desirable since our assumption could overestimate global NH_3 emissions.

Timing of N fertilizer application can also be a major factor that controls NH_3 volatilization from soils. Pinder *et al.* (2004) indicated that the greatest uncertainty in NH_3 missions are attributable to farming practices. In the DLEM, fertilizer was applied one to four times per year based on field experiments and literature review (Xu *et al.*, 2018). Except for China and North America, most regions had a one-time fertilizer application, which could introduce large uncertainties in global NH_3 emission estimates (Table S1). Furthermore, variation in N fertilizer application timing could affect monthly NH_3 emissions at regional scales. Xu *et al.* (2015) indicated higher NH_3 emissions in China during summer (June to August) and autumn (September to November) with a peak observed in July that was in agreement with findings of Zhang *et al.* (2011). However, those results were inconsistent with the seasonal emission patterns reported by Fu *et al.* (2015) and Huang *et al.* (2012). Fu *et al.* (2015) pointed out that difficulties capturing exact fertilization dates could cause the large discrepancy among studies on seasonal NH_3 estimates in China. Gilliland *et al.* (2003, 2006) investigated seasonal NH_3 emissions for the continental United States and found that emissions were highest in summer followed by spring since fertilizer application activity peaks during these seasons. Thus, since seasonal NH_3 emissions are heavily dependent on fertilizer application date, more information on fertilization timing from field operations is needed to minimize uncertainties.

This study provided evidence that climate change could significantly accelerate NH_3 emissions from agricultural systems. However, few studies have focused on NH_3 emissions under future conditions. Sutton *et al.* (2013) predicted that a 5°C warming could increase global NH_3 emissions by 40%. Sensitivity tests conducted by Riddick *et al.* (2016) also support potential accelerated global NH_3 emissions due to warming. However, those studies did not consider other factors that could affect NH_3 emissions from soils when attempting to predict the

responses of NH_3 emissions to global warming. In future work, a multi-factor environmental change framework is required to more accurately predict NH_3 emissions at global and regional scales.

Acknowledgements

This work has been supported by NSF grants (NSF1243232, NSF1243220), CAS grants (KFJ-STS-ZDTP-0; SKLURE2017-1-6), NOAA Grants (G00010410, G00010318), and AU-OUC Joint Center Program. We appreciate other members of Ecosystem Dynamics and Global Ecology (EDGE) Laboratory for their contribution to the development of DLEM model and global data sets. We thank two anonymous reviewers for their constructive comments. The model input and output data in this study are archived in International Center for Climate and Global Change Research at Auburn University (http://wp.auburn.edu/cgc/).

Reference

Alluvione F, Bertora C, Zavattaro L, Grignani C (2010) Nitrous oxide and carbon dioxide emissions following green manure and compost fertilization in corn. Soil Science Society of America Journal, **74**, 384-395.

Asman WA, Sutton MA, Schjørring JK (1998) Ammonia: emission, atmospheric transport and deposition. New phytologist, **139**, 27-48.

Aulakh MS, Khera TS, Doran JW, Bronson KF (2001) Denitrification, N_2O and CO_2 fluxes in rice-wheat cropping system as affected by crop residues, fertilizer N and legume green manure. Biology and Fertility of Soils, **34**, 375-389.

Bash J, Cooter E, Dennis R, Walker J, Pleim J (2013) Evaluation of a regional air-quality model with bidirectional NH 3 exchange coupled to an agroecosystem model. Biogeosciences, **10**, 1635-1645.

Behera SN, Betha R, Balasubramanian R (2013) Insights into chemical coupling among acidic gases, ammonia and secondary inorganic aerosols. Aerosol and Air Quality Research, **13**, 1282-U1414.

Beusen A, Bouwman A, Heuberger P, Van Drecht G, Van Der Hoek K (2008) Bottom-up uncertainty estimates of global ammonia emissions from global agricultural production systems. Atmospheric Environment, **42**, 6067-6077.

Bouwman A, Boumans L, Batjes N (2002) Estimation of global NH_3 volatilization loss from synthetic fertilizers and animal manure applied to arable lands and grasslands. Global biogeochemical cycles, **16**.

Bouwman A, Lee D, Asman W, Dentener F, Van Der Hoek K, Olivier J (1997) A global high‐resolution emission inventory for ammonia. Global biogeochemical cycles, **11**, 561-587.

Byun D, Schere KL (2006) Review of the governing equations, computational algorithms, and other components of the Models-3 Community Multiscale Air Quality (CMAQ) modeling system. Applied Mechanics Reviews, **59**, 51-77.

Ciais P, Sabine C, Bala G *et al.* (2014) Carbon and other biogeochemical cycles. In: *Climate Change 2013: The Physical Science Basis. Contribution of Working Group I to the Fifth Assessment Report of the Intergovernmental Panel on Climate Change*. Pp. 465-570, Cambridge University Press, Cambridge, UK

Dentener, F.: Global maps of atmospheric nitrogen deposition, 1860, 1993, and 2050, Data set, Oak Ridge National Laboratory Distributed Active Archive Center, Oak Ridge, Tennessee, USA, daac. ornl. gov, 2006.

Erisman JW, Sutton MA, Galloway J, Klimont Z, Winiwarter W (2008) How a century of ammonia synthesis changed the world. Nature Geoscience, **1**, 636-639.

FAO & IFA report (2001) *Global estimates of gaseous emissions of NH_3, NO and N_2O from agricultural land*. First version, Rome.

Fu X, Wang S, Ran L *et al.* (2015) Estimating NH_3 emissions from agricultural fertilizer application in China using the bi-directional CMAQ model coupled to an agro-ecosystem model. Atmospheric Chemistry and Physics, **15**, 6637-6649.

Gilliland AB, Appel KW, Pinder RW, Dennis RL (2006) Seasonal NH_3 emissions for the continental United States: Inverse model estimation and evaluation. Atmospheric Environment, **40**, 4986-4998.

Gilliland AB, Dennis RL, Roselle SJ, Pierce TE (2003) Seasonal NH_3 emission estimates for the eastern United States based on ammonium wet concentrations and an inverse modeling method. Journal of Geophysical Research: Atmospheres, **108**.

Goldewijk KK, Beusen A, Doelman J, Stehfest E (2017) Anthropogenic land use estimates for the Holocene–HYDE 3.2. Earth System Science Data, **9**, 927.

Gruber N, Galloway JN (2008) An Earth-system perspective of the global nitrogen cycle. Nature, **451**, 293-296.

Guy SO, Gareau RM (1998) Crop rotation, residue durability, and nitrogen fertilizer effects on winter wheat production. Journal of Production Agriculture, **11**, 457-461.

Heffer, P (2013), Assessment of fertilizer use by crop at the Clobal level 2010-2010/11, IFA, Paris, France.

Huang X, Song Y, Li M *et al.* (2012) A high-resolution ammonia emission inventory in China. Global biogeochemical cycles, **26**.

IPCC (2006) IPCC Guidelines for National Greenhouse Gas Inventories. *National Greenhouse Gas Inventories Programme (IGES)*, Japan.

Ju X-T, Xing G-X, Chen X-P *et al.* (2009) Reducing environmental risk by improving N management in intensive Chinese agricultural systems. Proceedings of the National Academy of Sciences, pnas. 0813417106.

Jung M, Henkel K, Herold M, Churkina G (2006) Exploiting synergies of global land cover products for carbon cycle modeling. Remote Sensing of Environment, **101**, 534-553.

Kunzová E, Hejcman M (2009) Yield development of winter wheat over 50 years of FYM, N, P and K fertilizer application on black earth soil in the Czech Republic. Field Crops Research, **111**, 226-234.

Liu M, Tian H (2010) China's land cover and land use change from 1700 to 2005: Estimations from high-resolution satellite data and historical archives. Global biogeochemical cycles, **24**.

Lopez-Bellido RJ, Lopez-Bellido L, Benítez-Vega J, Lopez-Bellido FJ (2007) Tillage system, preceding crop, and nitrogen fertilizer in wheat crop. Agronomy Journal, **99**, 59-65.

Lu C, Tian H (2013) Net greenhouse gas balance in response to nitrogen enrichment: perspectives from a coupled biogeochemical model. Global change biology, **19**, 571-588.

Lu C, Tian H (2017) Global nitrogen and phosphorus fertilizer use for agriculture production in the past half century: shifted hot spots and nutrient imbalance. Earth System Science Data, **9**, 181.

Lu C, Tian H, Liu M, Ren W, Xu X, Chen G, Zhang C (2012) Effect of nitrogen deposition on China's terrestrial carbon uptake in the context of multifactor environmental changes. Ecological Applications, **22**, 53-75.

Mahajan G, Chauhan B, Timsina J, Singh P, Singh K (2012) Crop performance and water-and nitrogen-use efficiencies in dry-seeded rice in response to irrigation and fertilizer amounts in northwest India. Field Crops Research, **134**, 59-70.

Massad R-S, Nemitz E, Sutton M (2010) Review and parameterisation of bi-directional ammonia exchange between vegetation and the atmosphere. Atmospheric Chemistry and Physics, **10**, 10359-10386.

Matthews E (1994) Nitrogenous fertilizers: global distribution of consumption and associated emissions of nitrous oxide and ammonia. Global biogeochemical cycles, **8**, 411-439.

Nemitz E, Sutton MA, Schjoerring JK, Husted S, Wyers GP (2000) Resistance modelling of ammonia exchange over oilseed rape. Agricultural and Forest Meteorology, **105**, 405-425.

590 Nishina K, Ito A, Hanasaki N, Hayashi S (2017) Reconstruction of spatially detailed global map of NH
591 4+ and NO 3-application in synthetic nitrogen fertilizer. Earth System Science Data, **9**, 149.
592 Olivier JG, Jjm B, Peters JA, Bakker J, Visschedijk AJ, Bloos JJ (2002) Applications of EDGAR
593 emission database for global atmospheric research.
594 Pan S, Tian H, Dangal SR *et al.* (2015) Responses of global terrestrial evapotranspiration to climate
595 change and increasing atmospheric CO_2 in the 21st century. Earth's Future, **3**, 15-35.
596 Pan S, Tian H, Dangal SR *et al.* (2014) Complex Spatiotemporal Responses of Global Terrestrial Primary
597 Production to Climate Change and Increasing Atmospheric CO_2 in the 21 st Century. PloS one, **9**,
598 e112810.
599 Pinder RW, Adams PJ, Pandis SN (2007) Ammonia emission controls as a cost-effective strategy for
600 reducing atmospheric particulate matter in the eastern United States. Environmental science &
601 technology, **41**, 380-386.
602 Pinder RW, Strader R, Davidson CI, Adams PJ (2004) A temporally and spatially resolved ammonia
603 emission inventory for dairy cows in the United States. Atmospheric Environment, **38**, 3747-3756.
604 Potter P, Ramankutty N, Bennett EM, Donner SD (2010) Characterizing the spatial patterns of global
605 fertilizer application and manure production. Earth Interactions, **14**, 1-22.
606 Rao V, Tooly L, Drukenbrod (2013) 2008 National emissions inventory: Review, analysis and highlights.
607 Reis S, Pinder R, Zhang M, Lijie G, Sutton M (2009) Reactive nitrogen in atmospheric emission
608 inventories. Atmospheric Chemistry and Physics, **9**, 7657-7677.
609 Ren W, Tian H, Tao B, Huang Y, Pan S (2012) China's crop productivity and soil carbon storage as
610 influenced by multifactor global change. Global Change Biology, **18**, 2945-2957.
611 Ren W, Tian H, Tao B *et al.* (2015) Large increase in dissolved inorganic carbon flux from the
612 Mississippi River to Gulf of Mexico due to climatic and anthropogenic changes over the 21st
613 century. Journal of Geophysical Research: Biogeosciences, **120**, 724-736.
614 Ren W, Tian H, Xu X *et al.* (2011) Spatial and temporal patterns of CO_2 and CH_4 fluxes in China's
615 croplands in response to multifactor environmental changes. Tellus B, **63**, 222-240.
616 Riddick S, Ward D, Hess P, Mahowald N, Massad R, Holland E (2016) Estimate of changes in
617 agricultural terrestrial nitrogen pathways and ammonia emissions from 1850 to present in the
618 Community Earth System Model. Biogeosciences, **13**, 3397-3426.
619 Sacks WJ, Deryng D, Foley JA, Ramankutty N (2010) Crop planting dates: an analysis of global patterns.
620 Global Ecology and Biogeography, **19**, 607-620.
621 Schlesinger WH, Hartley AE (1992) A global budget for atmospheric NH_3. Biogeochemistry, **15**, 191-
622 211.
623 Seinfeld J, Pandis S (1998) *Atmospheric Chemistry and Physics, 1326 pp*, John Wiley, Hoboken, NJ.

Sommer SG, Olesen JE (1991) Effects of dry matter content and temperature on ammonia loss from surface-applied cattle slurry. Journal of Environmental Quality, **20**, 679-683.

Sutton MA, Reis S, Riddick SN *et al.* (2013) Towards a climate-dependent paradigm of ammonia emission and deposition. Philosophical Transactions of the Royal Society of London B: Biological Sciences, **368**, 20130166.

Tian H, Banger K, Bo T, Dadhwal VK (2014) History of land use in India during 1880–2010: Large-scale land transformations reconstructed from satellite data and historical archives. Global and Planetary Change, **121**, 78-88.

Tian H, Chen G, Lu C *et al.* (2015) Global methane and nitrous oxide emissions from terrestrial ecosystems due to multiple environmental changes. Ecosystem Health and Sustainability, **1**, 1-20.

Tian H, Lu C, Chen G *et al.* (2012b) Contemporary and projected biogenic fluxes of methane and nitrous oxide in North American terrestrial ecosystems. Frontiers in Ecology and the Environment, **10**, 528-536.

Tian H, Lu C, Ciais P *et al.* (2016) The terrestrial biosphere as a net source of greenhouse gases to the atmosphere. Nature, **531**, 225-228.

Tian H, Lu C, Melillo J *et al.* (2012a) Food benefit and climate warming potential of nitrogen fertilizer uses in China. Environmental Research Letters, **7**, 044020.

Tian H, Xu X, Liu M, Ren W, Zhang C, Chen G, Lu C (2010) Spatial and temporal patterns of CH_4 and N_2O fluxes in terrestrial ecosystems of North America during 1979–2008: application of a global biogeochemistry model. Biogeosciences, **7**, 2673-2694.

Tian H, Xu X, Lu C *et al.* (2011) Net exchanges of CO_2, CH_4, and N_2O between China's terrestrial ecosystems and the atmosphere and their contributions to global climate warming. Journal of Geophysical Research: Biogeosciences, **116**.

USDA NASS https://quickstats.nass.usda.gov/

Wei Y, Liu S, Huntzinger D *et al.* (2013) The North American carbon program multi-scale synthesis and terrestrial model intercomparison project–part 2: environmental driver data. Geoscientific Model Development Discussions, **6**, 5375-5422.

Xu P, Liao Y, Lin Y *et al.* (2016) High-resolution inventory of ammonia emissions from agricultural fertilizer in China from 1978 to 2008. Atmospheric Chemistry and Physics, **16**, 1207-1218.

Xu P, Zhang Y, Gong W, Hou X, Kroeze C, Gao W, Luan S (2015) An inventory of the emission of ammonia from agricultural fertilizer application in China for 2010 and its high-resolution spatial distribution. Atmospheric Environment, **115**, 141-148.

Xu R, Pan S, Chen J et al. (2018) Half‐Century Ammonia Emissions From Agricultural Systems in Southern Asia: Magnitude, Spatiotemporal Patterns, and Implications for Human Health. GeoHealth, **2**, 40-53.

Xu R, Tian H, Lu C, Pan S, Chen J, Yang J, Bowen Z (2017) Preindustrial nitrous oxide emissions from the land biosphere estimated by using a global biogeochemistry model. Climate of the Past, **13**, 977.

Yan X, Akimoto H, Ohara T (2003) Estimation of nitrous oxide, nitric oxide and ammonia emissions from croplands in East, Southeast and South Asia. Global change biology, **9**, 1080-1096.

Yang Q, Tian H, Friedrichs MA, Hopkinson CS, Lu C, Najjar RG (2015) Increased nitrogen export from eastern North America to the Atlantic Ocean due to climatic and anthropogenic changes during 1901–2008. Journal of Geophysical Research: Biogeosciences, **120**, 1046-1068.

Zhang X, Davidson EA, Mauzerall DL, Searchinger TD, Dumas P, Shen Y (2015) Managing nitrogen for sustainable development. Nature, **528**, 51-59.

Zhang Y, Dore A, Ma L, Liu X, Ma W, Cape J, Zhang F (2010) Agricultural ammonia emissions inventory and spatial distribution in the North China Plain. Environmental Pollution, **158**, 490-501.

Zhang Y, Luan S, Chen L, Shao M (2011) Estimating the volatilization of ammonia from synthetic nitrogenous fertilizers used in China. Journal of environmental management, **92**, 480-493.

Zhou F, Ciais P, Hayashi K *et al.* (2016) Re-estimating NH_3 Emissions from Chinese Cropland by a New Nonlinear Model. Environmental science & technology, **50**, 564-572.

Zou J, Huang Y, Lu Y, Zheng X, Wang Y (2005) Direct emission factor for N_2O from rice–winter wheat rotation systems in southeast China. Atmospheric Environment, **39**, 4755-4765.

678 **Table 1.** Simulation experiment design in this study.

Experiments	Climate			Nitrogen Fertilizer	CO_2	LUC
	Source	Temperature	Precipitation			
Initial simulation	CRUNCEP	Averaged (1901–1930)	Averaged (1901–1930)	1900	1900	1900
S1	CRUNCEP	Averaged (1901–1930)	Averaged (1901–1930)	1901–2010	1901–2010	1901–2010
S2	CRUNCEP	1901–2010	Averaged (1901–1930)	1901–2010	1901–2010	1901–2010
S3	CRUNCEP	1901–2010	1901–2010	1901–2010	1901–2010	1901–2010
S4	WFDEI.GPCC	1901–2010	1901–2010	1901–2010	1901–2010	1901–2010
S5	GSWP3	1901–2010	1901–2010	1901–2010	1901–2010	1901–2010
S6	PGMFD v.2	1901–2010	1901–2010	1901–2010	1901–2010	1901–2010

679 **Table 2.** Estimates of global NH_3 emissions (expressed in Tg N yr^{-1}) based on different approaches.

Region	Year	Method	NH_3 emission	Reference
Global	2000	DLEM-Bi-NH_3	13.6 ± 0.5	This study*
	1995		12.4 ± 0.3	
	2000	IPCC Tier 1 guideline	7.7	IPCC, 2006
	2000	Process-based model	12.0	Riddick *et al.* (2016)
	1995	Constant EF	9.0	Bouwman *et al.* (2002)

680 * Mean ±2 standard deviation (s.d.) calculated from simulation results based on four different climate
681 datasets.

682

683 **Fig. 1** Simulated ammonia (NH_3) emissions in response to application of synthetic nitrogen (N) fertilizer
684 in: (a) the 1960s, (b) the 1980s, (c) the 1990s, and (d) the 2000s at a spatial resolution of 0.5 by 0.5 degree.

685

686 **Fig. 2** The continental-scale estimation of ammonia (NH_3) emission in the 1960s, the 1980s, the 1990s,
687 and the 2000s. Error bars, ±2 standard deviation (s.d.) calculated from simulation results based on four
688 different climate datasets. All units are Tg N yr^{-1}.

689

690 **Fig. 3** Simulated seasonal mean ammonia (NH_3) emissions in the 2000s: (a)
691 December–January–February, (b) March–April–May, (c) June–July–August, and (d)
692 September–October–November.

693

694 **Fig. 4** Crop-specific NH_3 emissions from synthetic N fertilizer application estimated by the DLEM-Bi-
695 NH_3 module (a) and the IPCC EF (b).

696

697 **Fig. 5** Climate effects on ammonia (NH_3) emissions during 1961–2010. The temperature impact on
698 annual NH_3 emissions was calculated through the difference between S2 and S1 experiments; the
699 precipitation impact on annual NH_3 emissions was calculated through the difference between S3 and S2
700 experiments; the temperature difference equals annual average temperature during 1961–2010 minus the
701 average temperature during 1901–1930.

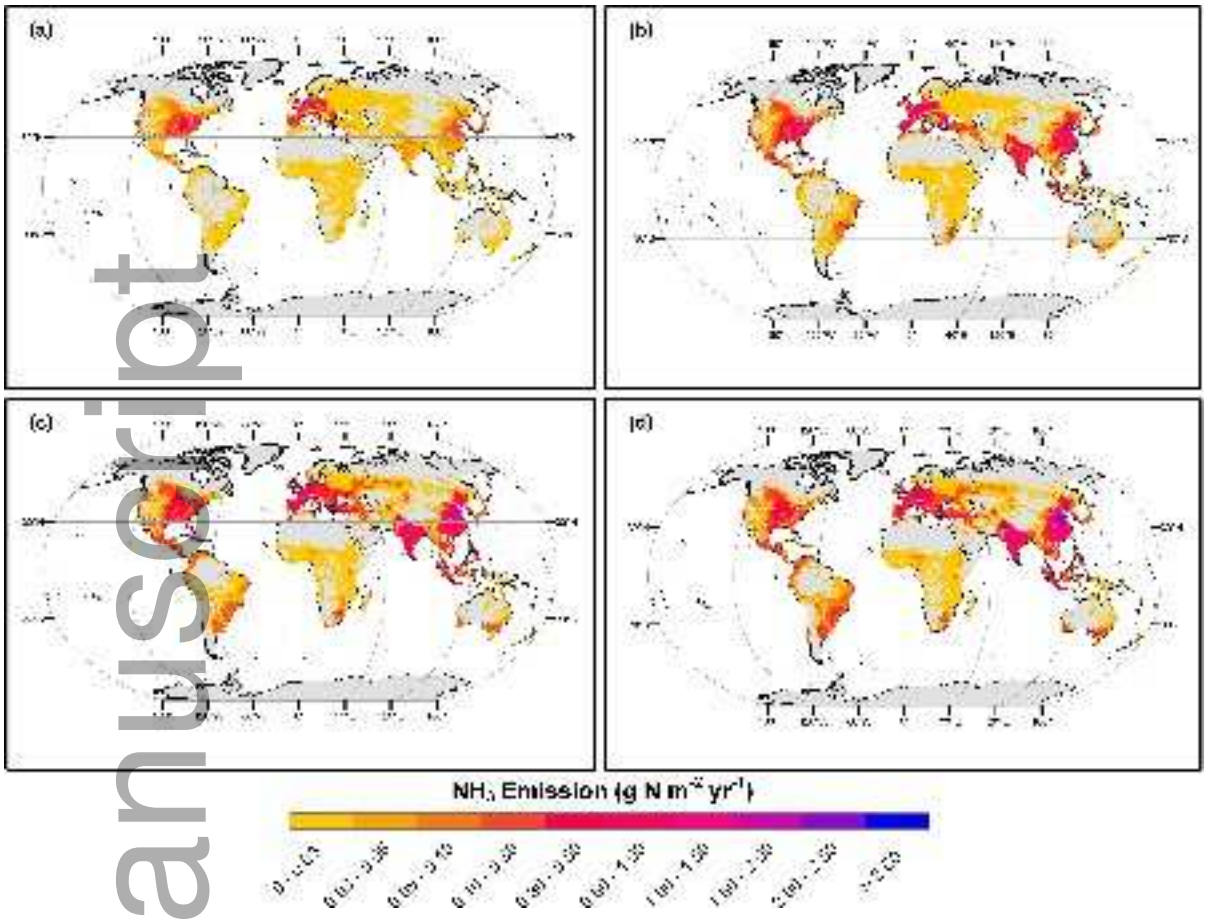

gcb_14499_f1.png

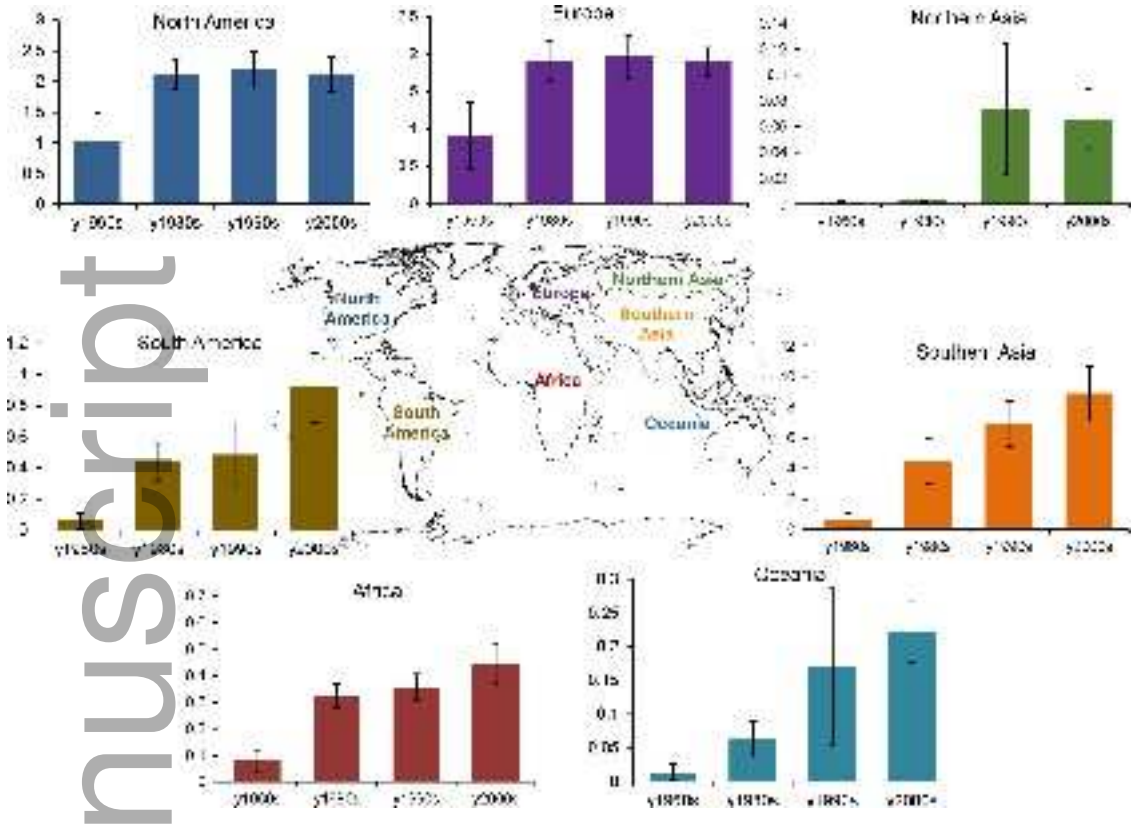

gcb_14499_f2.png

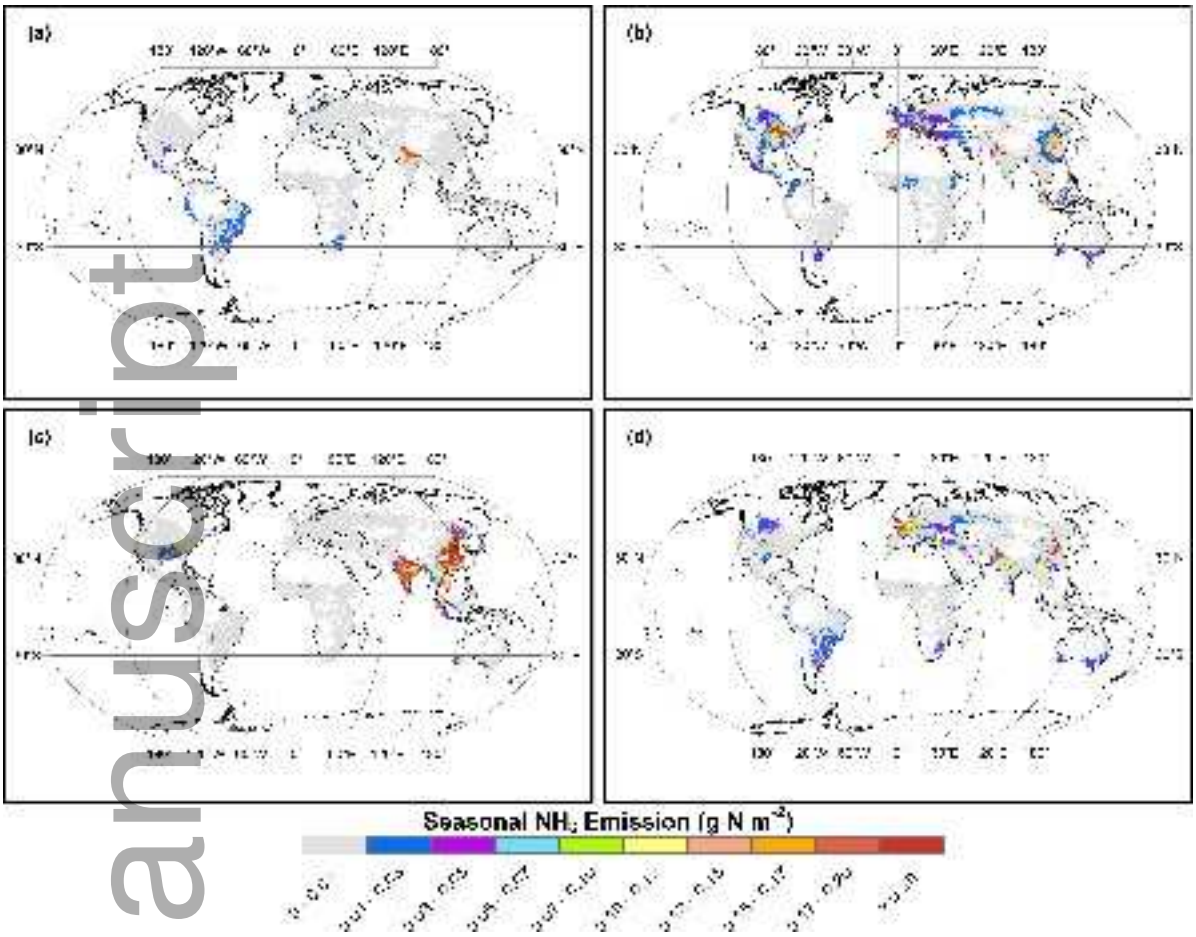

gcb_14499_f3.png

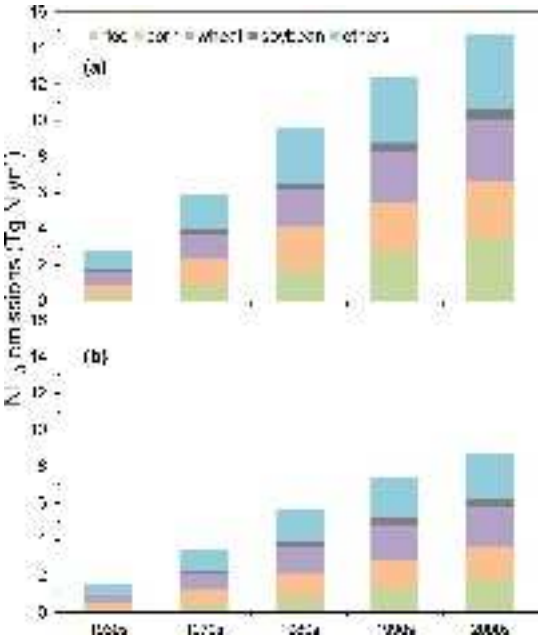

gcb_14499_f4.png

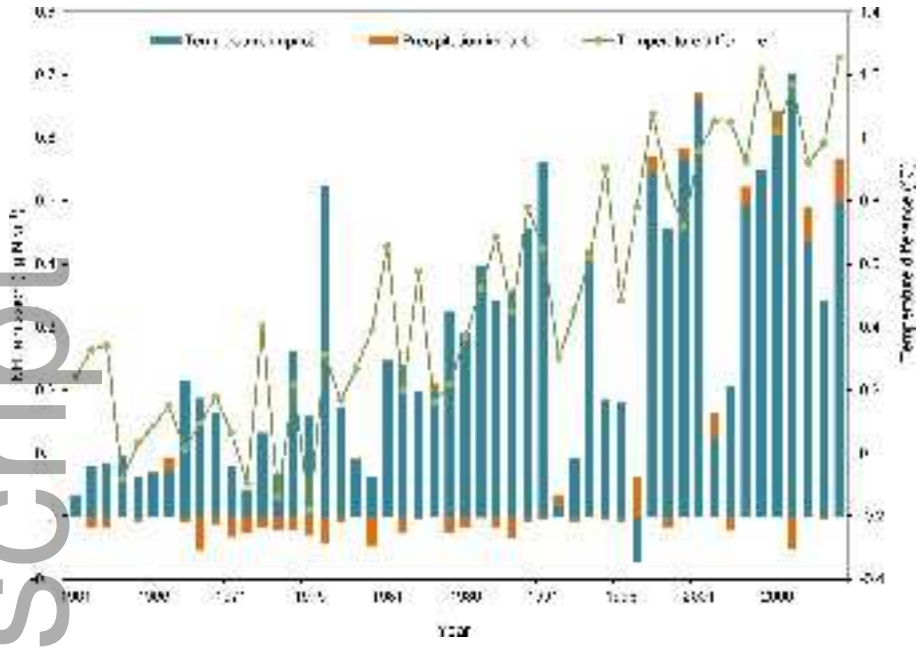

gcb_14499_f5.png